Nonparaxial tilted waveobjects

Alexandr B. Plachenov, Pedro Chamorro-Posada and Aleksei P. Kiselev

***Abstract*—Simple closed-form analytical expressions for tilted astigmatic wave beams and wavepackets that are exact solutions of the wave equation are constructed. They are obtained through two different but equivalent derivations, one is based on a complex shift in the Bateman-type solutions, the other employs their Lorentz transformation. Analytic expressions for the propagation invariants: energy, momentum and orbital angular momentum of tilted waveobjects with general astigmatism are presented.**

***Index Terms*—Nonparaxial wave propagation, tilted waveobjects, propagation invariants, orbital angular momentum.**

I. Introduction

ONE cannot overestimate the role played in modern science and technology by wave phenomena described by Gaussian-localized solutions of the wave equation

$$\Box u = \frac{1}{c^2} u_{tt} - u_{xx} - u_{yy} - u_{zz} = 0\,, \tag{1}$$

$c = \mathrm{const}$. The mainstream basic approach to such processes still rests on an approximate theory based on the parabolic equation. However, along with this well-established paraxial framework, in the 1980s certain exact solutions of Eq. (1) were introduced that describe Gaussian wave beams and packets, see, e.g. [1]–[5]. Both theories employ fairly similar mathematical structures, among which the *phase function* plays an outstanding role.

Within the paraxial theory of localized waveobjects, propagation is restricted to angles very close to that fixed by a particular axis. Even though *tilted* beams and packets can be addressed with this approximate approach, these must propagate at a small angle to this fundamental direction, named optical axis in the context of optics. We will also stand by this convention in spite of the broader scope of our work.

In the series of papers [6]–[8], an important class of tilted wave beams was thoroughly investigated. The main motivation for the introduction of these solutions was the accurate and convenient analysis of propagation and scattering problems when the boundary plane of the aperture field is non-orthogonal to the optical axis. In their detailed study of such solutions, Hadad and Melamed [6]–[8] proposed a specific version of the paraxial theory for which the *tilt angle* between the direction of beam propagation and the optical axis may be not small, although the angular distribution of the beam is still assumed to be narrow. Paraxial tilted beams were addressed in [9] where they were employed in a trick allowing novel higher-order modes by integrating over the complexifying parameter.

In contrast to this previous research, we address *exact* solutions of the wave equation, having similar properties but not subject to the conditions of paraxiality that imply the smallness of tilt angles and angular spectral widths. We develop a further generalization of the well-known relatively undistorted solutions containing a functional parameter that determines the nature of the localization of the function under consideration. These solutions can be shaped as time-inharmonic and spatially inclined beams and packets, whose properties will be investigated in detail. In particular, we will show that a beam can have a propagation direction distinct of that of its own axis and that the isoamplitude surfaces of a packet are approximately ellipsoids with axes non-trivially oriented with respect to direction of propagation.

Our main technical tool is a complex shift with the transverse variables in the fundamental astigmatic mode solution [5]. Looking at the matter broadly, it should be noted that the direct use of complex shift to study localized solutions of the wave equation goes back to Hillion [10], who applied it to a longitudinal variable in the classical Bateman solution [11], [12]. As a result, he arrived at the Bateman–Hillion class of relatively undistorted waves [3], [4], which contains a rich set of Gaussian localized beam-like and packet-like solutions with axisymmetric phases. This class was extended in our paper [5] by considering astigmatic phases.

The complex shift in solutions of the wave equation was discussed in detail for the 2D case in [13]. Some preliminary results were mentioned in a short conference paper note [14]. The tilted fundamental mode seemingly first appeared (with no discussion) for axisymmetric case in the course of a systematic formal consideration of Helmholtz-Gauss higher-order modes both in paraxial [15] and in exact theory [16].

In this work, we also describe an alternative derivation of these tilted solutions based on the observation of the equivalence between a complex shift in the transverse coordinates and the combination of a Lorentz transformation and a rotation. A similar idea can be found in [17], devoted to the theory of 2D Poincaré wavelets.

We present analytical expressions for the conserved quantities of Eq. (1): energy, momentum and angular momentum of tilted beams and packets including those with general astigmatism. The derivation is mediated by the exploration

Alexandr B. Plachenov is with MIREA – Russian Technological University, 78 Vernadsky Avenue, Moscow, 119454, Russia. (e-mail: a_plachenov@mail.ru).

Pedro Chamorro-Posada is with Dpto. de Teoría de la Señal y Comunicaciones e Ingeniería Telemática, Universidad de Valladolid, Paseo Belén n^o 15, 47011 Valladolid, Spain. (e-mail: pedcha@tel.uva.es).

Aleksei P. Kiselev is with St. Petersburg Department of V.A. Steklov Mathematical Institute, Fontanka 27, 191023, St.Petersburg, Russia, and Institute for Problems in Mechanical Engineering of the Russian Academy of Sciences, V.O., Bolshoj pr., 61, 199178, St.Petersburg, Russia. (e-mail: aleksei.kiselev@gmail.com)

P.C-P. acknowledges support from the Spanish Ministerio de Ciencia e Innovación (MCIN), project PID2020-119418GB-I00, and with funding from the European Union NextGenerationEU (PRTRC17.I1) and the Consejería de Educación, Junta de Castilla y León, through QCAYLE project.

A.P.K. acknowledges the support from Russian Science Foundation, grant 22-11-00338, in obtaining the results of Sections IV and VII.

of the properties of our solutions in their asymptotic limits.

II. Non-tilted astigmatic Bateman solutions

We start with the formulation of astigmatic Bateman-type exact solutions of Eq. (1) introduced in [5] and describing highly localized non-tilted wave beams and wave packets.

A. Relatively undistorted progressing waves

We note that all the solutions of the equation (1) we are dealing with fall under the classical definition of *relatively undistorted progressive waves* [18], i.e., they have the form

$$u = gf(\theta)\,, \tag{2}$$

where the *amplitude* $g = g(x, y, z, t)$ and the *phase* $\theta = \theta(x, y, z, t)$ are fixed functions, and the *waveform* f is an arbitrary function of one variable. Thus, (2) describes in fact a family of solutions with a functional parameter f. Generally speaking, functions f, g and θ can be real or complex. In the latter case both real and imaginary parts of u are solutions of (1) as well.

B. Bateman-type solutions with a general astigmatic phase

We set the z-axis as the optical axis of the system and we call the Cartesian coordinate z the longitudinal variable. The characteristic variables

$$\alpha = z - ct\,, \qquad \beta = z + ct \tag{3}$$

are related, respectively, to forward and backward wave propagation along the z-axis. By $\mathbf{r} = \binom{x}{y}$ we denote the 2D vector of transverse coordinates, and by $\mathbf{r}^T = (x, y)$ its transpose.

In [5], certain solutions were introduced closely related to paraxial astigmatic fundamental modes [19] and characterized by the *complexified astigmatic Bateman phase*

$$\theta = \alpha + \mathbf{r}^T \mathbf{\Gamma}(\beta)\mathbf{r}\,, \tag{4}$$

where $\mathbf{\Gamma}(\beta)$ is a 2×2 symmetric matrix with positive definite imaginary part. The matrix $\mathbf{\Gamma}$ is thus parameterized by 6 free real constants. Being a phase in the above sense, its dependence on β obeys the equation [5]

$$\mathbf{\Gamma}^{-1}(\beta) = \mathbf{\Gamma}_0^{-1} + \beta\mathbf{I}\,, \tag{5}$$

where $\mathbf{\Gamma}_0^{-1} = \mathbf{\Gamma}^{-1}(0)$, and $\mathbf{I}$ is the 2×2 unit matrix. Therefore, $\operatorname{Im}\mathbf{\Gamma}_0^{-1} = \operatorname{Im}\mathbf{\Gamma}^{-1}(\beta)$ is negative definite, then the matrix $\operatorname{Im}\mathbf{\Gamma}(\beta)$ is positive definite, whence the phase takes the values in the closed complex upper half-plane $\mathbb{C}_+$,

$$\operatorname{Im}\theta \geq 0. \tag{6}$$

The phase is real only when $\mathbf{r} = 0$ i.e. on the z-axis.

It is important to note that since the phase (4) is complex, the waveform $f(\theta)$ must be an analytic function (see [20]) in $\mathbb{C}_+$.

We confine our consideration to the case where the amplitude g is independent of the transverse variables $\mathbf{r}$. As shown in [5], it only differs from

$$g = \sqrt{\det\mathbf{\Gamma}(\beta)} \tag{7}$$

by a constant factor.

The ansatz (2) with the phase (4) and the amplitude (7) is a solution of the wave equation (1). By analogy with the paraxial case, this solution is called the *fundamental astigmatic mode*. Under a proper choice of the waveform f it can describe non-paraxial time-dependent Gaussian beams (known in the axisymmetric case as focus wave beams [1]) and Gaussian wave packets, see [3] and section II-D.

Aiming exclusively at the description of solutions localized near the z-axis, we note that they must decrease with distance from the axis. This is equivalent to assume[1] that

$$f(\theta) \to 0 \ \text{ as } \ \operatorname{Im}\theta \to \infty. \tag{8}$$

C. Special cases of astigmatism

In the case where $\mathbf{\Gamma}$ is diagonal,

$$\mathbf{\Gamma}(\beta) = \operatorname{diag}[(\beta - z_1 - ib_1)^{-1}, (\beta - z_2 - ib_2)^{-1}] \tag{9}$$

and $z_{1,2}$ and $b_{1,2}$ are real constants, $b_{1,2} > 0$, expression (2),(4),(7) reduces to the simple astigmatic (for $z_1 \neq z_2$ and/or $b_1 \neq b_2$) solution [3]. The degenerate case where $z_1 = z_2 = 0$ and $b_1 = b_2 = b$, i.e.,

$$\mathbf{\Gamma}(\beta) = (\beta - ib)^{-1}\mathbf{I} \tag{10}$$

is that of complexified axisymmetric (stigmatic) Bateman–Hillion phase first introduced in [10]. For simple astigmatic phase (9) Eq. (7) reduces (up to a constant factor) to

$$g = \frac{1}{\sqrt{\beta - z_1 - ib_1}\sqrt{\beta - z_2 - ib_2}}, \tag{11}$$

and for the axisymmetric phase (10) – to

$$g = \frac{1}{\beta - ib}. \tag{12}$$

If we perform the rotation in xy-plane, then the matrix $\mathbf{\Gamma}(\beta)$ for simple astigmatic phase becomes nondiagonal. Putting formally the rotation angle in such matrix nonreal, we come to Arnaud-Kogelnik general astigmatic phase [19]. Further, in the course of numerical calculations, we'll use the letter Ψ for imaginary part of the rotation angle [5].

D. Waveforms of particular interest

The above assumption $\operatorname{Im}\mathbf{\Gamma}(\beta) > 0$ implies that $\operatorname{Im}\theta \geq 0$, and the waveform f can be taken as an arbitrary function of a complex variable analytic in the closed upper half-plane $\mathbb{C}_+$. We are interested only in those waveforms that rapidly decrease as $|\mathbf{r}|$ grows and demonstrate beam-like or packetlike behavior of the solution.

We will pay a special attention to two particular waveforms:

$$f(\theta) = \exp(ik\theta) \tag{13}$$

with k a real constant, and

$$f(\theta) = \exp\left[2ka\left(1 - \sqrt{1 - i\theta/a}\right)\right] \tag{14}$$

[1] It follows from the maximum modulus principle for analytic functions [21] asserting that the maximum of the modulus of an analytic function bounded in the domain (in our case it is $\mathbb{C}_+$) is attained at the boundary (in our case it is the real axis).

with k and a real constants. Following [2], [3] we take the branch of the square root having positive imaginary part.

The waveform (13) is associated with a Gaussian beam and in the axisymmetric case it reduces to the focus wave mode [1], whereas (14) is associated with a simple Gaussian wave packet [2], [3]. On the upper half-plane $\mathbb{C}_+$, the function (13) is strongly localized near the real axis $\operatorname{Im}\theta = 0$ where its modulus equals to one. The modulus of (14) is one at $\theta = 0$, at all other points of $\mathbb{C}_+$ it is smaller and, as shown in [2], [3], exponentially decays when $|\theta| \to \infty$.

III. Complex shift

Translation symmetry of the wave equation (1) allows shifts, both real and complex, with respect to transverse variables. In this section we describe an approach to the construction of tilted solutions via such a shift.

Let $\mathbf{r}^*$ be an arbitrarily fixed complex 2D vector. Making the shift

$$\mathbf{r} \mapsto \mathbf{r} - \mathbf{r}^* \tag{15}$$

in the generalized Bateman solution (2) with (4) and (7) we arrive at a solution of Eq. (1), having the form of relatively undistorted progressing wave (2) with the phase

$$\theta^* = \alpha + (\mathbf{r} - \mathbf{r}^*)^T \mathbf{\Gamma}(\beta)(\mathbf{r} - \mathbf{r}^*) \tag{16}$$

and the same amplitude.

After some algebra, see Appendix A, we represent function (16) in the form convenient for further analysis:

$$\theta^* = \theta_2 + \theta_1 + \theta_0, \tag{17}$$

with

$$\theta_2 = (\mathbf{r} - \mathbf{r}_0 - \beta\boldsymbol{\tau}\tan\phi)^T \mathbf{\Gamma}(\beta)(\mathbf{r} - \mathbf{r}_0 - \beta\boldsymbol{\tau}\tan\phi)\,, \tag{18}$$

$$\theta_1 = \frac{z\cos 2\phi + \boldsymbol{\tau}^T(\mathbf{r} - \mathbf{r}_0)\sin 2\phi - ct}{\cos^2\phi}\,, \tag{19}$$

$$\theta_0 = \boldsymbol{\tau}^T \mathbf{\Gamma}_0^{-1} \boldsymbol{\tau} \tan^2\phi\,. \tag{20}$$

Here, the angle ϕ, the real unit transverse vector $\boldsymbol{\tau}$ and the real transverse vector $\mathbf{r}_0$ are expressible via $\mathbf{\Gamma}_0$ and $\mathbf{r}^*$, see (100),(102) but they can be treated alternatively as new independent parameters.

As we have earlier noted, the waveform $f(\theta)$ of a complexified Bateman solution is analytic on the upper half-plane. However, the function $\operatorname{Im}\theta^*$ may take negative values (because $\operatorname{Im}\theta_0 < 0$) where $f(\theta^*)$ is not defined. To avoid this trouble we henceforth put in (2) $\theta = \theta^* - \theta_0$, i.e.,

$$\theta = \theta_1 + \theta_2\,. \tag{21}$$

and consider the solution of (1) of the form

$$u = \sqrt{\det \mathbf{\Gamma}(\beta)}\, f(\theta)\,. \tag{22}$$

Also, it is convenient to perform an additional real shift of the coordinate system in the xy plane and a rotation about the z axis, as a result of which the vector $\mathbf{r}_0$ vanishes and the direction of the vector $\boldsymbol{\tau}$ coincides with the direction of the x-axis. In what follows, we will assume that such transformations are completed which gives

$$\theta_1 = \frac{1}{\cos^2\phi}[(z - ct\cos 2\phi)\cos 2\phi + (x - ct\sin 2\phi)\sin 2\phi]\,, \tag{23}$$

$$\theta_2 = \boldsymbol{\rho}^T \mathbf{\Gamma}(\beta)\boldsymbol{\rho}, \tag{24}$$

where

$$\boldsymbol{\rho} = \mathbf{r} - \beta\boldsymbol{\tau}\tan\phi = (x - \beta\tan\phi, y)^T\,. \tag{25}$$

IV. Lorentz transformations

Here, we describe an alternative derivation of the above tilted solutions based on the classical Lorentz transformation [22].

A solution of the wave equation (1) in a reference frame with space-time variables $t, \mathbf{R}$, $\mathbf{R} = (x, y, z)^T = (\mathbf{r}, z)^T$ can be expressed in a second frame $t', \mathbf{R}'$, moving at a constant velocity to the former, using the the Lorentz transformation

$$t' = \frac{t - \mathbf{v}^T\mathbf{R}/c^2}{\sqrt{1 - |\mathbf{v}|^2/c^2}}\,, \mathbf{R}' = \frac{\mathbf{R} - \mathbf{v}t}{\sqrt{1 - |\mathbf{v}|^2/c^2}}\,. \tag{26}$$

Here, $\mathbf{v}$ is a 3D real speed vector $|\mathbf{v}| < c$ specifying the velocity of the primed Cartesian frame measured in the unprimed frame. We now consider separately longitudinal (Lorentz boosts) and transverse Lorentz transforms.

A. Longitudinal Lorentz transformation

Start with the case of $\mathbf{v}$ directed along the z-axis, where $\mathbf{r}' = \mathbf{r}$,

$$t' = \frac{t - vz/c^2}{\sqrt{1 - (v/c)^2}}\,, z' = \frac{z - vt}{\sqrt{1 - (v/c)^2}}\,, \tag{27}$$

$$\alpha' = \sqrt{\frac{c - v}{c + v}}\alpha = \lambda\alpha\,,\ \beta' = \sqrt{\frac{c + v}{c - v}}\beta = \frac{\beta}{\lambda}\,. \tag{28}$$

Here, v is a projection of $\mathbf{v}$ on the z-axis. The number $\lambda = \sqrt{\frac{c-v}{c+v}}$ may be greater than or less than one depending on the sign of v. We come up with a new relatively undistorted wave solution of the form (2), (4), (7) with g, θ and $\mathbf{\Gamma}$ replaced by the respective primed functions defined as follows

$$\theta' = \lambda\alpha + \mathbf{r}^T \mathbf{\Gamma}\left(\frac{\beta}{\lambda}\right)\mathbf{r} = \lambda[\alpha + \mathbf{r}^T \mathbf{\Gamma}'(\beta)\,\mathbf{r}]\,, \tag{29}$$

$$g' = \sqrt{\det \mathbf{\Gamma}\left(\frac{\beta}{\lambda}\right)}\,, \tag{30}$$

and

$$\mathbf{\Gamma}'(\beta) = \frac{1}{\lambda}\mathbf{\Gamma}\left(\frac{\beta}{\lambda}\right)\,. \tag{31}$$

The latter formula will be needed below.

B. Transverse Lorentz transformation

Now let the unit real vector $\boldsymbol{\tau}$ be orthogonal to the z axis and, for simplicity, we take $\boldsymbol{\tau} = (1,0)^T$. It is convenient to define the vector $\mathbf{v}$ in (26) by $\mathbf{v} = c\boldsymbol{\tau}\sin\phi$, where ϕ is a certain angle (which, as will be seen from what follows, will have the same meaning as earlier, see (18)-(20)). The Lorentz transformation (26) allows $z' = z$, $y' = y$,

$$t' = \frac{t - x\sin\phi/c}{\cos\phi}\,,\ x' = \frac{x - ct\sin\phi}{\cos\phi}\,, \tag{32}$$

$$\alpha' = \frac{z\cos\phi + x\sin\phi - ct}{\cos\phi}\,,\ \beta' = \frac{z\cos\phi - x\sin\phi + ct}{\cos\phi}. \tag{33}$$

Let us show that these transformations give the results identical to that obtained earlier. We make a rotation of the axes of the initial variables:

$$\tilde z = z\cos\phi - x\sin\phi\,,\quad \tilde x = x\cos\phi + z\sin\phi\,,\quad \tilde t = t\,,$$
$$z = \tilde z\cos\phi + \tilde x\sin\phi\,,\quad x = \tilde x\cos\phi - \tilde z\sin\phi\,,\quad y' = y = \tilde y\,,$$

whence

$$x' = \frac{\tilde x\cos\phi - \tilde z\sin\phi - c\tilde t\sin\phi}{\cos\phi} = \tilde x - (\tilde z + c\tilde t)\tan\phi\,,$$
$$\alpha' = \frac{\tilde z\cos 2\phi + \tilde x\sin 2\phi - c\tilde t}{\cos\phi}\,,\quad \beta' = \frac{\tilde z + c\tilde t}{\cos\phi}$$

Denote $\tilde\beta = \tilde z + c\tilde t$, $\tilde{\mathbf{r}} = \binom{\tilde x}{\tilde y}$, then

$$\beta' = \frac{\tilde\beta}{\cos\phi}\,, \tag{34}$$

$$\mathbf{r}' = \begin{pmatrix} x' \\ y' \end{pmatrix} = \tilde{\mathbf{r}} - \tilde\beta\boldsymbol{\tau}\tan\phi =: \tilde{\boldsymbol{\rho}}\,. \tag{35}$$

Now we express the non-tilted phase (4) presented in Lorentz-transformed variables through the rotated variables $\tilde x$, $\tilde y$, $\tilde z$ and $\tilde t$. After an elementary, although cumbersome algebra we obtain the expression for the new phase

$$\begin{aligned}\theta' &= \alpha' + \mathbf{r}'^T\boldsymbol{\Gamma}(\beta')\mathbf{r}' \\ &= \frac{\tilde z\cos 2\phi + \tilde x\sin 2\phi - ct}{\cos\phi} \\ &\quad + (\tilde{\mathbf{r}} - \tilde\beta\boldsymbol{\tau}\tan\phi)^T\boldsymbol{\Gamma}\left(\frac{\tilde\beta}{\cos\phi}\right)(\tilde{\mathbf{r}} - \tilde\beta\boldsymbol{\tau}\tan\phi) \\ &= \cos\phi\left[\frac{\tilde z\cos 2\phi + \tilde x\sin 2\phi - ct}{\cos^2\phi} + \tilde{\boldsymbol{\rho}}^T\tilde{\boldsymbol{\Gamma}}(\tilde\beta)\tilde{\boldsymbol{\rho}}\right]\,,\end{aligned} \tag{36}$$

with

$$\tilde{\boldsymbol{\Gamma}}(\tilde\beta) = \frac{1}{\cos\phi}\boldsymbol{\Gamma}\left(\frac{\tilde\beta}{\cos\phi}\right)\,. \tag{37}$$

The formula (37) will coincide with (31) if we put $\lambda = \cos\phi$.

To summarize, we observe that the formulas of section III found via complex transverse shift can be alternatively obtained by successful application of
1) longitudinal Lorentz transformation with $\lambda = \cos^{-1}\phi$,
2) rotation in xz plane by the angle ϕ and
3) transverse Lorentz transformation in x-direction with the speed $v = c\sin\phi$.

V. Properties of the tilted astigmatic phase

A. The phase at moderate values of coordinates and time

Consider now the properties of the tilted phase given by (21). The function θ_1 is a linear real function of x and y, and its surface levels are planes that move with the speed c at the angle 2ϕ to the z-axis. The function θ_2 is quadratic in $\mathbf{r}$, its imaginary part $\operatorname{Im}\theta_2$ is nonnegative and vanishes when $\mathbf{r} = \beta\boldsymbol{\tau}\tan\phi$, i.e.

$$x = (z + ct)\tan\phi\,,\qquad y = 0\,. \tag{38}$$

At each instant of time t it is a straight line, which is tilted at an angle ϕ to z-axes. The level surfaces of $\operatorname{Im}\theta_2$ and $\operatorname{Re}\theta_2$ move with a speed c along the z-axis in the negative direction.

Let the phase (21) be real and fix its value. The points where this value retains are those of intersection of the straight line $\theta_2 = 0$ (38) which we call the beam axis, and a certain plane $\theta_1 = \text{const}$. These points run with the speed c, the direction of propagation lie in the xz-plane, the angle between the speed vector and the z-axis is equal to 2ϕ.

Let us now fix the instant of time t and consider the surface where the value of $\operatorname{Im}\theta = \operatorname{Im}\theta_2$ is constant:

$$\boldsymbol{\rho}^T\operatorname{Im}\boldsymbol{\Gamma}(\beta)\boldsymbol{\rho} = \text{const}\ . \tag{39}$$

In the stigmatic case (10), such a surface is a one-sheeted hyperboloid, but in the general case, it is not a surface of the second order. However, the sections of such a surface by the planes $z = \text{const}$ are always ellipses whose centers lie on the line (38), and directions and lengths of the semiaxes depend on z.

Confining the consideration to the case where $\boldsymbol{\tau}$ is parallel to the x-axis, we get

$$\boldsymbol{\rho} = \mathbf{r} - \beta\boldsymbol{\tau}\tan\phi = (\check x/\cos\phi, \check y)$$

where

$$\check x = x\cos\phi - (z + ct)\sin\phi\,,\qquad \check y = y$$

are the Cartesian coordinates in the plane orthogonal to the line (38). It is seen that the surface (39) is flattened in the plane xz by a factor of $\cos\phi$ as compared with a similar surface for the non-tilted phase for the same matrix $\boldsymbol{\Gamma}(\beta)$.

Let us now turn to the surfaces $\operatorname{Re}\theta = \text{const}$, which we will call *fronts*. Their shapes are quite intricate even in the case of a non-shifted phase. However, we are interested in the behavior of solutions of (1) for small $\boldsymbol{\rho}$, where the terms quadratic in $\boldsymbol{\rho}$ are relatively small. Since $\operatorname{Re}\theta_2$ depends quadratically on the transverse coordinates, the main term here turns out to be a linear function θ_1, and at points lying on (38), the level lines of this function are tangent planes to the fronts. The distinguishing feature of the phase (21) is that the fronts are no longer orthogonal to the line (38) as it was in the non-tilted case, and they intersect it at an angle $\frac{\pi}{2} - \phi$.

Consider the moving point $\mathbf{M} \in \mathbb{R}^3$ described by

$$x = ct\sin 2\phi\,,\ y = 0\,,\ z = ct\cos 2\phi\,, \tag{40}$$

where $\theta = \theta_1 = \theta_2 = 0$. At each instant of time, the straight line (38) and the plane $\theta_1 = 0$ intersect at $\mathbf{M}$. It moves along

with this plane at the speed c in the direction forming the angle 2ϕ with the z axis, always remaining in the xz plane.

Further it will be convenient to use the Cartesian coordinates rotated relative to the original system (x, y, z) by an angle 2ϕ

$$\hat{x} = -z\sin 2\phi + x\cos 2\phi\,,\ \hat{y} = y\,,\ \hat{z} = z\cos 2\phi + x\sin 2\phi, \tag{41}$$

in which the direction of the axis $\hat{z}$ coincides with the direction of motion of the point **M**. In these coordinates, the expression for the phase (21) takes the form

$$\theta = \theta_1 + \theta_2 = \frac{\hat{z} - ct}{\cos^2\phi} + \boldsymbol{\rho}^T\boldsymbol{\Gamma}(\beta)\boldsymbol{\rho}\,, \tag{42}$$

where

$$\beta = \hat{z}\cos 2\phi - \hat{x}\sin 2\phi + ct\,, \quad \boldsymbol{\rho} = (\hat{x} + (\hat{z} - ct)\tan\phi, \hat{y})^T\,.$$

B. The phase at large values of coordinates and time

Consider first the phase (21) in the case when either time or distance is large. It is immediately seen from (42) that at any fixed point both $\operatorname{Re}\theta$ and $\operatorname{Im}\theta$ tend to infinity as t becomes large. Similarly, at any fixed instant of time $\operatorname{Re}\theta$ grows infinitely with $R = \sqrt{x^2 + y^2 + z^2}$, but $\operatorname{Im}\theta$ tends to infinity with $|\boldsymbol{\rho}|$, that is with the distance from the beam axis (38).

We now address the case of the coordinated tendency of both distance and time to infinity, which is important for what follows. Let both ct and R tend to infinity, provided that their difference

$$s = R - ct$$

remains limited, which condition we present as follows

$$s = O(1),\ ct \to +\infty. \tag{43}$$

Such asymptotics of the non-tilted Bateman-type solutions for the axisymmetric case were found in [2], [3].

The asymptotics of θ depends on the direction in which the observation point

$$\mathbf{R} = (ct + s)\mathbf{n} \tag{44}$$

moves, where $\mathbf{n} = \mathbf{R}/R$ is the unit vector directed from the origin to $\mathbf{R}$. If $\mathbf{n}$ is opposite to the direction of the z-axis, then β remains limited, as does $\operatorname{Im}\theta$, while $\operatorname{Re}\theta \to \infty$. For all other directions $\beta \to \infty$.

First, we observe that, for large values β, the formula (5) implies

$$\boldsymbol{\Gamma}(\beta) = \left(\boldsymbol{\Gamma}_0^{-1} + \beta\mathbf{I}\right)^{-1} \approx \mathbf{I}/\beta - \boldsymbol{\Gamma}_0^{-1}/\beta^2. \tag{45}$$

Therefore,

$$\theta_2 = \boldsymbol{\rho}^T\boldsymbol{\Gamma}(\beta)\boldsymbol{\rho} \approx |\boldsymbol{\rho}|^2/\beta - \boldsymbol{\rho}^T\boldsymbol{\Gamma}_0^{-1}\boldsymbol{\rho}/\beta^2\,. \tag{46}$$

The use of the definition of $\boldsymbol{\rho}$ (25) yields

$$\frac{|\boldsymbol{\rho}|^2}{\beta} = \frac{x^2 + y^2}{\beta} - 2x\tan\phi + (z + ct)\tan^2\phi \tag{47}$$

for the first term on the right-hand side of (46).

Thence, the expression (23) for θ_1 is easily transformed to

$$\theta_1 = (z - ct) + 2x\tan\phi - (z + ct)\tan^2\phi. \tag{48}$$

With the observation that $z - ct = (z^2 - c^2t^2)/\beta$, we obtain from (46), (47) and (48) for large values of β the approximation

$$\theta = \theta_1 + \theta_2 \approx \frac{R^2 - c^2t^2}{\beta} - \frac{\boldsymbol{\rho}^T\boldsymbol{\Gamma}_0^{-1}\boldsymbol{\rho}}{\beta^2}.$$

With a small difficulty, we find the limit function to which θ tends as $\beta \to \infty$,

$$\theta((ct + s)\mathbf{n}, t) \to \Theta, \tag{49}$$

$$\Theta = \Theta(s, \mathbf{n}) = \Theta_1 + \Theta_2\,, \tag{50}$$

where Θ_1 is linear with respect to s, and Θ_2 is independent of s and is approximately quadratic in distance from the beam axis:

$$\Theta_1 = \Theta_1(s, \mathbf{n}) = 2hs\,, \tag{51}$$

$$\Theta_2 = \Theta_2(s) = -h^2\sin^2\chi\boldsymbol{\psi}^T\boldsymbol{\Gamma}_0^{-1}\boldsymbol{\psi}\,. \tag{52}$$

Here, $\boldsymbol{\psi}$ is the 2D vector defined by

$$\boldsymbol{\psi} = (\cos\varphi - \tan(\chi/2)\tan\phi, \sin\varphi)^T\,, \tag{53}$$

and

$$h = h(\mathbf{n}) = \frac{1}{1 + \cos\chi\cos 2\phi - \sin\chi\cos\varphi\sin 2\phi}\,. \tag{54}$$

We use spherical angular coordinates (χ, φ) with the polar axis along the $\hat{z}$-axis (41):

$$\hat{x} = R\sin\chi\,\cos\varphi\,, \quad \hat{y} = R\sin\chi\sin\varphi\,, \quad \hat{z} = R\cos\chi\,,$$

$0 \le \chi \le \pi$, $-\pi < \varphi \le \pi$. Where $\mathbf{n}$ is opposite to the direction of the z-axis, i.e., at $\chi = \pi - 2\phi$, $\varphi = 0$, the functions h and Θ turn to infinity.

It deserves to be mentioned that though the splitting of the phase Θ into a sum (50) is somewhat similar to representation (42), neither Θ_1 is the limit of θ_1, nor $\theta_2 \to \Theta_2$.

VI. Tilted solutions with particular waveforms

A. Gaussian beams

Let us move on to considering solutions of the wave equation (1) of the form (22) with the waveform (13):

$$\begin{aligned} u &= \sqrt{\det\boldsymbol{\Gamma}(\beta)}\exp(ik\theta) \\ &= \exp\left(\frac{ik}{\cos^2\phi}(z\cos 2\phi + x\sin 2\phi - ct)\right) \\ &\qquad \times \sqrt{\det\boldsymbol{\Gamma}(\beta)}\exp\left(ik\boldsymbol{\rho}^T\boldsymbol{\Gamma}(\beta)\boldsymbol{\rho}\right)\,. \end{aligned} \tag{55}$$

The first factor on the right-hand side is a plane wave corresponding to the wavenumber $k\cos^{-2}\phi$ and propagating under the angle 2ϕ with the axis z. Other two factors represent a Gaussian beam whose axis (38) is tilted by the angle ϕ at the z-axis. Modulus of the solutions (55) is given by

$$\begin{aligned} |u| &= \sqrt{|\det\boldsymbol{\Gamma}(\beta)|}\exp(-k\operatorname{Im}\theta_2) \\ &= \sqrt{|\det\boldsymbol{\Gamma}(\beta)|}\exp\left(-k\boldsymbol{\rho}^T\operatorname{Im}\boldsymbol{\Gamma}(\beta)\boldsymbol{\rho}\right)\,. \end{aligned} \tag{56}$$

Solution (55) is not square integrable and has an infinite energy.

B. Gaussian wavepackets at moderate values of coordinates and time

Consider the waveform $f(\theta)$ given by (14), for which in [3] is shown that (8) holds and the modulus of function

$$u = \sqrt{\det \mathbf{\Gamma}(\beta)} \exp\left[2ka\left(1 - \sqrt{1 - i\theta/a}\right)\right] \tag{57}$$

attains its maximum at the moving point $\mathbf{M}$ described by (40). At this point, the maximum value of the modulus of function f equals to one, and the solution (57) becomes

$$u|_{\mathbf{R}=\mathbf{M}} = \sqrt{\det \mathbf{\Gamma}(B)} \tag{58}$$

with $B = \beta|_{\mathbf{R}=\mathbf{M}} = 2ct\cos^2\phi$.

The structure of the function (57) around the point (40) depends on the values of the parameters k, a and the matrix $\mathbf{\Gamma}(\beta)$ and changes with time.

Solution (57) is square integrable and its energy is finite.

For moderate values of t and k, a both large which ensures a strong localization of the solution around $\mathbf{M}$, we, analogously to the consideration of the non-tilted axisymmetric solutions in [2], [3], expand the square root in powers of θ and obtain

$$2ka\left(1 - \sqrt{1 - i\theta/a}\right) \approx k\left(i\theta - \theta^2/4a\right) \approx k\left(i\theta - \theta_1^2/4a\right) , \tag{59}$$

which is true wherever the solution is not exponentially small. Omitting higher order term allows for (40) near $\mathbf{M}$ the expression

$$u \approx \sqrt{\det \mathbf{\Gamma}(B)} \exp(ik\theta_1) \exp\left[k\left(i\theta_2 - \theta_1^2/4a\right)\right] , \tag{60}$$

where θ_1 and θ_2 given by (42) with $\beta = B$. There, the exponent of the second exponential in (60) is a quadratic form with respect to deviations of Cartesian coordinates of observation point $\mathbf{R}$ from $\mathbf{M}$, its real part is negative definite. The modulus level surfaces of (60) are ellipsoids described by

$$\boldsymbol{\rho}^T \operatorname{Im} \mathbf{\Gamma}(B) \boldsymbol{\rho} + \frac{\theta_1^2}{4a} = \text{const} .$$

We note that principal axes of these ellipsoids are parallel neither to coordinate axes, nor to the straight line (38), nor to the trajectory of the point $\mathbf{M}$. In the process of the packet propagation, directions of such axes rotate together with the directions of principal axes of the matrix $\operatorname{Im} \mathbf{\Gamma}$.

These features are illustrated in Figures 1, 2 and 5, which displays the space-time evolution of untilted and tilted beam-like and packet-like solutions. Similar plots for solutions with general astigmatism are shown in Figures 3, 4 and 6. The visible distinction of some level surfaces from ellipsoids is observed far from the moving point $\mathbf{M}$.

As it was shown in [5], the above beam and packet solutions near $\mathbf{M}$ are related in such a way that the beam acts as the envelope of the corresponding packet in their respective spatiotemporal evolution. Such feature is illustrated in Figure 7 that shows corresponding beams and packets both in the tilted and non tilted case.

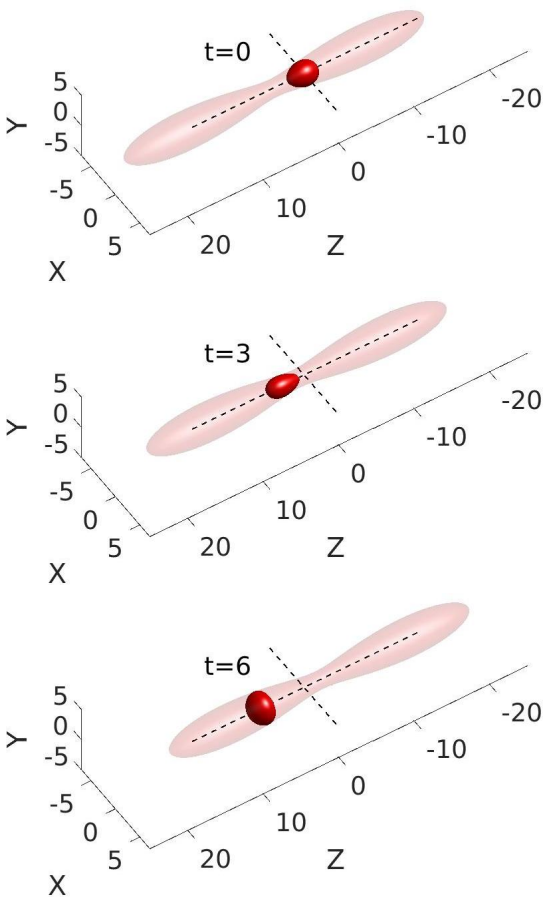

Fig. 1: Level surfaces of $|u|$ for an untilted Gaussian stigmatic packet and the amplitude of the corresponding beam at different times. $z_1 = z_2 = 4$, $b_1 = b_2 = 3$, and $k = 5$.

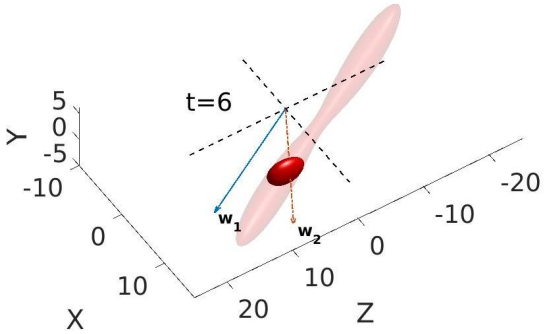

Fig. 2: Level surfaces of $|u|$ for a tilted Gaussian stigmatic packet and the amplitude of the corresponding beam at different times. $\phi = \pi/6$, $z_1 = z_2 = 4$, $b_1 = b_2 = 3$, and $k = 5$. Vectors $\mathbf{w}_1 = 20\boldsymbol{\tau}$ and $\mathbf{w}_2 = 20\mathbf{e}_s$ indicate the respective directions of vectors $\boldsymbol{\tau}$ and the unit speed vector $\mathbf{e}_s$.

C. Gaussian wavepackets at large values of coordinates and time

If either R or t is large, the phase (21) tends to infinity whence the solution (22) is exponentially small.

Assume now that R and t grow in such a way that the condition (43) is satisfied. If $\mathbf{n}$ is opposite to the direction

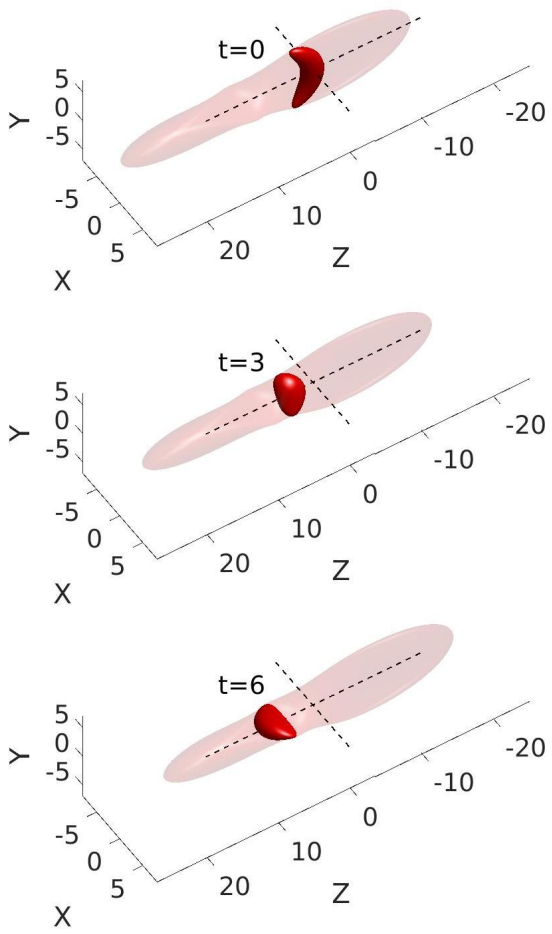

Fig. 3: Level surfaces of $|u|$ for an untilted GA packet and the amplitude of the corresponding beam at different times. $z_1 = 3$, $z_2 = 10$, $b_1 = 4$, $b_2 = 1$, $k = 5$ and $\Psi = 0.15$.

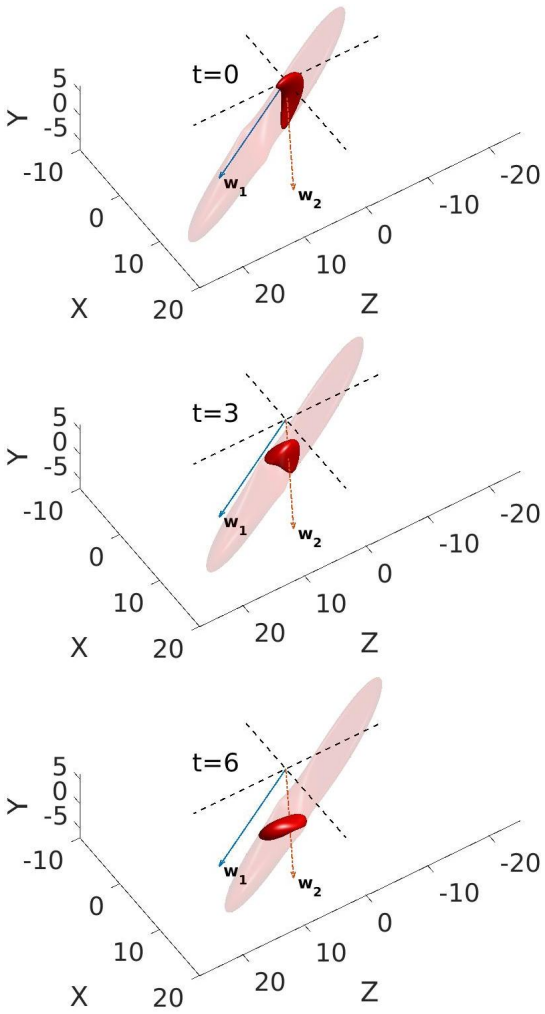

Fig. 4: Level surfaces of $|u|$ for a tilted GA packet and the amplitude of the corresponding beam at different times. $\phi = \pi/6$, $z_1 = 3$, $z_2 = 10$, $b_1 = 4$, $b_2 = 1$, $k = 5$ and $\Psi = 0.15$. Vectors $\mathbf{w}_1 = 20\boldsymbol{\tau}$ and $\mathbf{w}_2 = 20\mathbf{e}_s$ indicate the respective directions of vectors $\boldsymbol{\tau}$ and the unit speed vector $\mathbf{e}_s$.

of the z-axis, then $\beta = const$, and $\theta \to \infty$, whence the solution (22) exponentially decays. At all other directions of $\mathbf{n}$, $\theta \to \Theta(s, \mathbf{n})$, and $\beta \approx R/h(\mathbf{n})$, and, as seen from (10), the asymptotics of the amplitude (7) is $\sqrt{\det \mathbf{\Gamma}(\beta)} \approx h(\mathbf{n})/R$. Therefore,

$$u \approx \frac{h(\mathbf{n})}{R} f(\Theta(s, \mathbf{n})) \approx \frac{h(\mathbf{n})}{ct} f(\Theta(s, \mathbf{n}))\,, \qquad (61)$$

with $\Theta(s, \mathbf{n}) = \Theta(R - ct, \mathbf{n})$ given by (50). For the waveform (14), the function (61) exponentially decreases as $|s|$ grows, see [3].

Similarly to (59), we find that near the maximum modulus of the solution,

$$2ka\left(1 - \sqrt{1 - i\theta/a}\right) \approx k\left(i\Theta - \Theta_1^2/4a\right). \qquad (62)$$

The function Θ_1 is real and vanishes at $s = 0$, i.e., on the sphere $R = ct$. The function Θ_2 is complex with $\operatorname{Im}\Theta_2 \geq 0$ and vanishes at $\chi = 0$. In a neighborhood of the moving point $\mathbf{M}$ characterized by $s = 0$, $\chi = 0$, at which $\Theta = 0$, we hold the terms quadratic in s and χ, which gives

$$\Theta(s, \mathbf{n}) \approx 2h_0 s - h_0^2 \chi^2 \boldsymbol{\psi}_0^T \mathbf{\Gamma}_0^{-1} \boldsymbol{\psi}_0 \qquad (63)$$

where

$$\boldsymbol{\psi}_0 = (\cos\varphi, \sin\varphi)^T\,,\ h_0 = \frac{1}{1 + \cos 2\phi} = \frac{1}{2\cos^2\phi}\,. \qquad (64)$$

Thence,

$$u((ct + s)\mathbf{n}, t) \approx \frac{h_0}{ct} \exp(2ikh_0 s) \times \exp\left\{kh_0^2\left[-i\chi^2 \boldsymbol{\psi}_0^T \mathbf{\Gamma}_0^{-1} \boldsymbol{\psi}_0 - s^2/a\right]\right\}, \qquad (65)$$

which is applicable at large k where u is not exponentially small.

Further, we will be confined to large values of β which occurs at all directions $\mathbf{n}$ except the one opposite to the direction of the z-axis, where $z = -(ct + s)$ and $\beta = -s$ does not grow with time. There $\sqrt{\det \mathbf{\Gamma}(\beta)}$ does not vanish, but the waveform exponentially tends to zero. Therefore we neglect contribution of a small neighborhood of this direction to integrals describing energy, momentum and OAM.

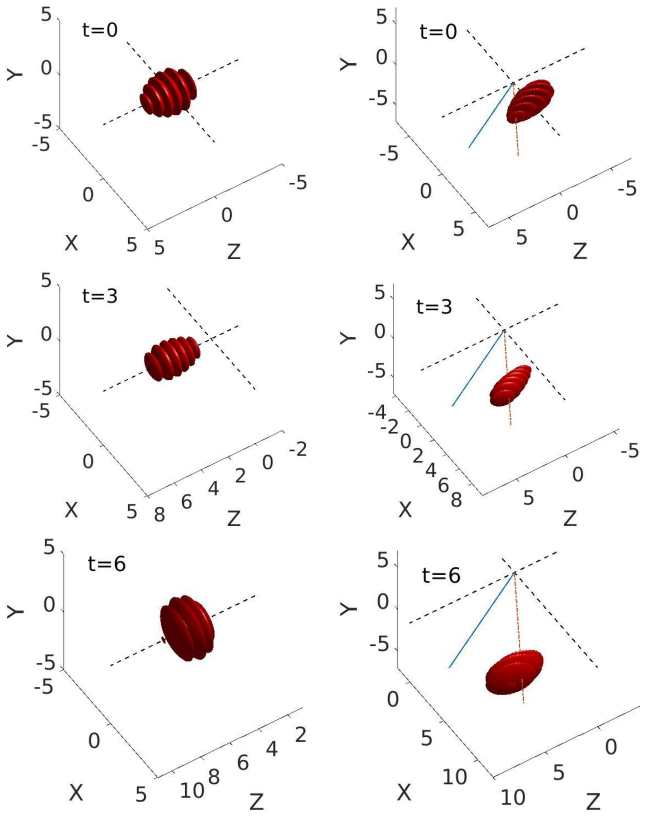

Fig. 5: Level surfaces of the real part of a Gaussian stigmatic packet at different times. Untilted $\phi = 0$ solutions are displayed on the left column. The corresponding tilted solutions with $\phi = \pi/6$ are shown on right column. In all cases, $z_1 = z_2 = 4$, $b_1 = b_2 = 3$, and $k = 5$. Solid blue and dashed-dote red lines indicate the respective directions of $\boldsymbol{\tau}$ and the speed vector.

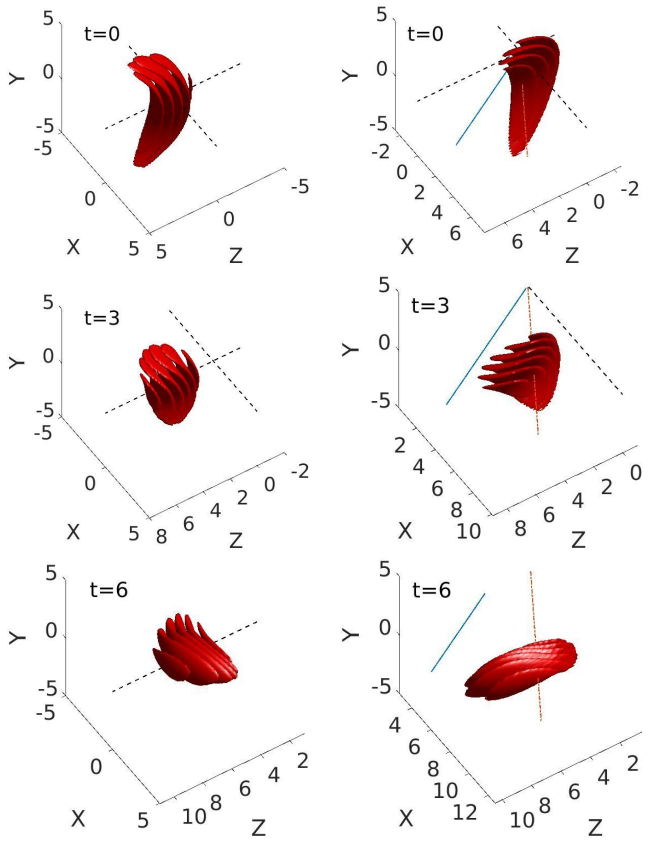

Fig. 6: Level surfaces of the real part of the a GA packet at different times. Untilted $\phi = 0$ solutions are displayed on the left column. The corresponding tilted solutions with $\phi = \pi/6$ are shown on right column. In all cases, $z_1 = 3$, $z_2 = 10$, $b_1 = 4$, $b_2 = 1$, $k = 5$ and $\Psi = 0.15$. Solid blue and dashed-dote red lines indicate the respective directions of $\boldsymbol{\tau}$ and the speed vector.

VII. Energy and momentum of a tilted wavepacket

In this section, we derive the analytic expressions for the first two conserved quantities of the wave equation (1), namely, the energy E and momentum $\mathbf{P}$, for a tilted wavepacket solution. We employ their independence on time for a convenient calculation in the asymptotic limit. In what follows, the waveform $f(\theta)$ is assumed to be strongly localized with respect to θ, that is, with respect to $\alpha = z - ct$, x, and y for moderate values of t, and with respect to $s = R - ct$ and χ for large t.

A. A general wavepacket

In this subsection, we do not presume any specific expression for the waveform which must be just localized to allow the convergence of the arising integrals. The leading terms of derivatives of (61) in the area (43) are given by differentiating only the waweform $f(\Theta)$. Introducing the notation

$$df(\Theta)/d\Theta := \dot{f}(\Theta)$$

and observing that $\partial\Theta(s,\chi,\varphi)/\partial s = 2h$, we find the approximations

$$\frac{1}{c}u_t \approx \frac{-2h^2}{R}\dot{f}(\Theta)\ , \nabla u \approx \frac{2h^2}{R}\dot{f}(\Theta)\,\mathbf{n}. \tag{66}$$

The expressions for energy density and for momentum density [23], [24] are

$$\mathcal{E} = \frac{1}{2}\left(|\nabla u|^2 + \frac{1}{c^2}|u_t|^2\right) \approx \frac{2h^4}{R^2}|\dot{f}(\Theta)|^2 \tag{67}$$

and

$$\boldsymbol{\mathcal{P}} = -\frac{1}{2c^2}\,\mathrm{Re}(u_t \nabla u^*) \approx \frac{2h^4}{cR^2}|\dot{f}\,(\Theta)\,|^2\mathbf{n}. \tag{68}$$

The star in (68) denotes complex conjugation. Here, we have noted that $|h| = h$ and replaced ct by R, which is approximately correct in the area (43). For an acoustic wavepacket, the energy and momentum of the sound wave are obtained multiplying Eqs. (67) and (68) by ρ_0, the density of the fluid at rest.

Energy $E = \iiint_{\mathbb{R}^3} \mathcal{E}\, d^3\mathbf{R}$ and momentum $\mathbf{P} = \iiint_{\mathbb{R}^3} \boldsymbol{\mathcal{P}}\, d^3\mathbf{R}$ are independent of time and can be conveniently found via integration of the respective densities at large t. The integrands are small outside the area (43) which allows

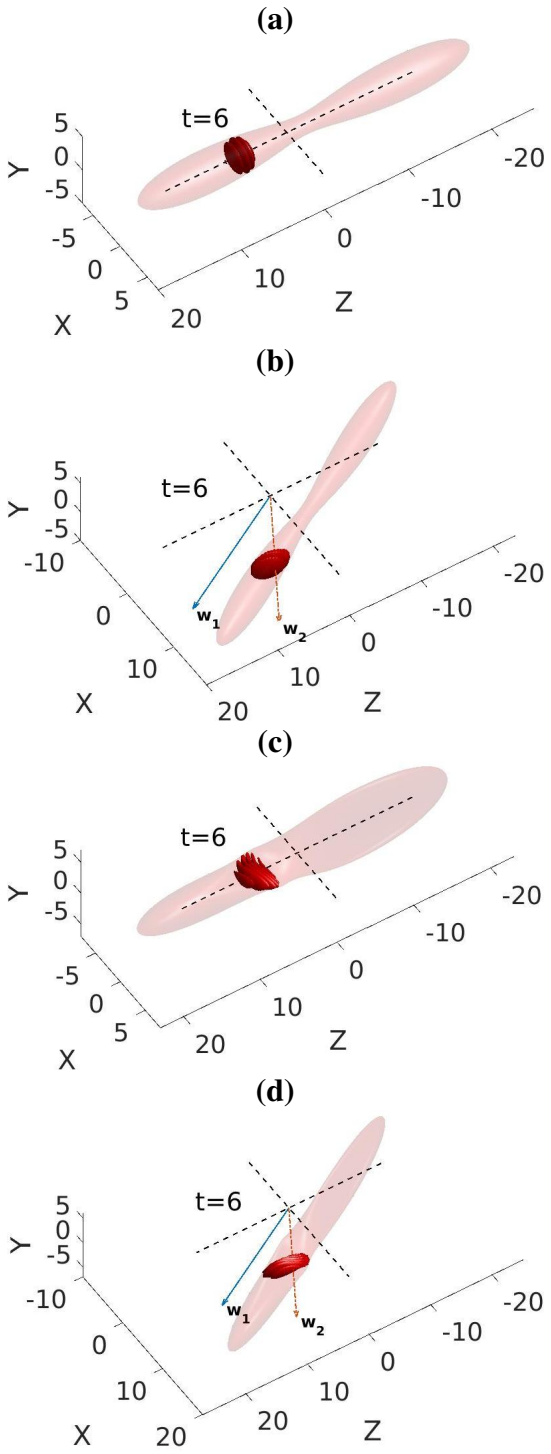

Fig. 7: Level surfaces of the real part of the GA packet and isosurfaces of the corresponding beams $|u|$ at $t = 6$. (a) and (c) are untilted solutions. (b) and (d) are tilted solutions with $\phi = \pi/6$. (a) and (b) are stigmatic solutions with $z_1 = z_2 = 4$, $b_1 = b_2 = 3$, and $k = 5$. (c) and (d) are solutions with general astigmatism with $z_1 = 3$, $z_2 = 10$, $b_1 = 4$, $b_2 = 1$, $k = 5$ and $\Psi = 0.15$.

us to integrate the expressions (67) and (68) over the entire space. We write the volume element as $dxdydz \equiv d^3\mathbf{R} = R^2 d^2\mathbf{n} dR = R^2 \sin\chi d\chi d\varphi dR$, denoting by $d^2\mathbf{n}$ the area element of the unit sphere S^2. Integration over R turns into integration over s. We obtain:

$$E = 4 \iint_{S^2} h^4(\mathbf{n})\, d^2\mathbf{n} \int_{-\infty}^{\infty} |\dot{f}(\Theta(s,\mathbf{n}))|^2\, ds, \tag{69}$$

$$\mathbf{P} = \frac{2}{c} \iint_{S^2} h^4(\mathbf{n})\, \mathbf{n}\, d^2\mathbf{n} \int_{-\infty}^{\infty} |\dot{f}(\Theta(s,\mathbf{n}))|^2\, ds. \tag{70}$$

In the axisymmetric case, the momentum $\mathbf{P}$ is parallel to the $\hat{z}$-axis.

B. The Gaussian wavepacket (14) *at large values of* k

Next, we will address the above specific Gaussian wavepacket under the condition that k is large. We will employ the observation that $\operatorname{Im}\Theta \geq 0$ and the absolute values of integrands in (69) in (70) reach sharp maxima where the arguments of exponentials in (59) vanish. As was shown in section VI-C, this occurs where $\chi = 0$ and $s = 0$. Assuming s and χ small, and using the notation (64), we get from (62)

$$|\dot{f}(\Theta)|^2 \approx k^2 \exp\left\{2kh_0^2\left[\chi^2 \boldsymbol{\psi}_0^T \operatorname{Im}\boldsymbol{\Gamma}_0^{-1}\boldsymbol{\psi}_0 - s^2/a\right]\right\}. \tag{71}$$

From (69) we obtain

$$E \approx 4k^2h_0^4 \iint_{S^2} \exp\left[2kh_0^2\chi^2\boldsymbol{\psi}_0^T \operatorname{Im}\boldsymbol{\Gamma}_0^{-1}\boldsymbol{\psi}_0\right] d^2\mathbf{n} \tag{72}$$

$$\times \int_{-\infty}^{+\infty} \exp\left[-2kh_0^2 s^2/a\right] ds\,. \tag{73}$$

Noting that

$$\int_{-\infty}^{\infty} \exp(-ms^2) ds = \sqrt{\pi/m}, \tag{74}$$

we replace the inner integral by $\sqrt{\pi a}/\sqrt{2k}h_0$ and come up with

$$E = 4k^2h_0^4 \frac{\sqrt{\pi a}}{\sqrt{2k}h_0} \int_0^{\pi} \chi\, d\chi \int_{-\pi}^{\pi} d\varphi \exp\left[2kh_0^2\chi^2\boldsymbol{\psi}_0^T \operatorname{Im}\boldsymbol{\Gamma}_0^{-1}\boldsymbol{\psi}_0\right]. \tag{75}$$

We extend with a small error the integration with respect χ and φ to the whole plane. Using the formula (see, e.g., [25])

$$\iint_{\mathbb{R}^2} \exp\left(-\mathbf{r}^T\mathbf{A}\mathbf{r}\right) d^2\mathbf{r} = \frac{\pi}{\sqrt{\det\mathbf{A}}} \tag{76}$$

allows

$$E \approx 4k^2h_0^4 \cdot \frac{\pi}{2kh_0^2\sqrt{\det\operatorname{Im}\boldsymbol{\Gamma}_0^{-1}}} \cdot \frac{\sqrt{\pi a}}{\sqrt{2k}h_0} =$$

$$= \frac{\pi^{3/2}}{\cos^2\phi}\sqrt{\frac{ka}{2\det\operatorname{Im}\boldsymbol{\Gamma}_0^{-1}}}. \tag{77}$$

Similarly, for momentum we obtain from (70)

$$\mathbf{P} \approx \frac{\pi^{3/2}}{2c\cos^2\phi}\sqrt{\frac{ka}{2\det\operatorname{Im}\boldsymbol{\Gamma}_0^{-1}}}\mathbf{n}_0\,, \tag{78}$$

where $\mathbf{n}_0$ is the unit vector along the $\hat{z}$ axis.

VIII. Orbital angular momentum of a tilted wavepacket

A. Orbital angular momentum in the general case

The density of angular momentum with respect to the $\hat{z}$-axis is [23], [24]

$$\mathcal{J} = -\frac{1}{2c}\operatorname{Re}(u_\varphi^* u_t). \tag{79}$$

Calculating the derivative u_φ in the area (43), which requires taking into account the dependencies on φ of both phase and amplitude, gives:

$$u_\varphi \approx -\frac{h^2\sin^2\chi}{R}(\boldsymbol{\psi}^T\boldsymbol{\Gamma}_0^{-1}\boldsymbol{\psi})_\varphi \dot{f}(\Theta) + u_h h_\varphi\,, \tag{80}$$

where

$$\begin{aligned}&(\boldsymbol{\psi}^T\boldsymbol{\Gamma}_0^{-1}\boldsymbol{\psi})_\varphi\\ &= 2(-\sin\varphi\,,\,\cos\varphi)\boldsymbol{\Gamma}_0^{-1}(\cos\varphi + \tan(\chi/2)\tan\phi\,,\,\sin\varphi)^T\,,\end{aligned} \tag{81}$$

and

$$h_\varphi = -h^2\sin\chi\sin\varphi\sin 2\phi\,. \tag{82}$$

Further,

$$u_h \approx \frac{h}{R}\dot{f}(\Theta)\cdot\Theta_h + \frac{1}{R}f(\Theta)\,, \tag{83}$$

where

$$\Theta_h = 2s - 2h\sin^2\chi\boldsymbol{\psi}^T\boldsymbol{\Gamma}_0^{-1}\boldsymbol{\psi}\,. \tag{84}$$

Employing (66) we get the expression for the OAM $J = \iiint_{\mathbb{R}^3}\mathcal{J}d^3\mathbf{R}$ in the form of a sum:

$$J = \frac{1}{c}(I_1 + I_2 + I_3), \tag{85}$$

$$I_1 = -\iint_{S^2} h^5\sin^2\chi[\boldsymbol{\psi}^T\operatorname{Re}\boldsymbol{\Gamma}_0^{-1}\boldsymbol{\psi}]_\varphi\, d^2\mathbf{n}\int_{-\infty}^{\infty}|\dot{f}(\Theta(s,\mathbf{n}))|^2\,ds, \tag{86}$$

$$I_2 = \iint_{S^2} h^3 h_\varphi\, d^2\mathbf{n}\times\int_{-\infty}^{\infty}|\dot{f}(\Theta(s,\mathbf{n}))|^2\operatorname{Re}\Theta_h\,ds, \tag{87}$$

$$I_3 = \iint_{S^2} h^2 h_\varphi\, d^2\mathbf{n}\int_{-\infty}^{\infty}\operatorname{Re}(\dot{f}(\Theta(s,\mathbf{n}))f^*(\Theta(s,\mathbf{n})))\,ds\,. \tag{88}$$

Note that $I_3 = 0$, which follows from the observation that

$$2h\operatorname{Re}(\dot{f}(\Theta(s,\mathbf{n}))f^*(\Theta(s,\mathbf{n}))) = (|f(\Theta(s,\mathbf{n}))|^2)_s\,,$$

whence the inner integral over s in (88) vanishes in virtue of the rapid decrease of the waveform at infinity. So, in general

$$J = \frac{1}{c}(I_1 + I_2)\,. \tag{89}$$

Under the additional assumption

$$|f(\operatorname{Re}\Theta + i\operatorname{Im}\Theta)| = |f(-\operatorname{Re}\Theta + i\operatorname{Im}\Theta)| \tag{90}$$

valid for the Gaussian-packet waveform (14), the expression for I_2 allows simplification. Indeed

$$\operatorname{Re}\Theta_h = \frac{\operatorname{Re}\Theta}{h} - h\sin^2\chi\boldsymbol{\psi}^T\operatorname{Re}\boldsymbol{\Gamma}_0^{-1}\boldsymbol{\psi}\,, \tag{91}$$

which allows us to replace $\operatorname{Re}\Theta_h$ in the inner integral in (87) by the second term on the right-hand side of (91). We come up with formula (89) where I_1 is given by (86) and

$$\begin{aligned}I_2 = \iint_{S^2} h^6\sin^3\chi\sin\varphi\sin 2\phi\,\boldsymbol{\psi}^T\operatorname{Re}\boldsymbol{\Gamma}_0^{-1}\boldsymbol{\psi}\,d^2\mathbf{n}\\ \times\int_{-\infty}^{\infty}|\dot{f}(\Theta(s,\mathbf{n}))|^2\,ds.\end{aligned} \tag{92}$$

B. The Gaussian wavepacket (14) at large values of k

As in the previous section, for the waveform (14), the approximation (71) shows that for large k, the integrands in (86) and (87) are localized at small values of χ. Since the integrand in (87) contains an additional multiplier $\sin\chi$ compared to (86), vanishing near the maximum point, we conclude that for large k,

$$|I_2| \ll |I_1|,$$

and I_2 in (89) can be neglected. As a result of calculations the details of which are given in Appendix B, we find the asymptotics of the integral (86) and obtain:

$$J \approx \frac{1}{c}\frac{\pi^{3/2}(\mu_1-\mu_2)\sin 2\varkappa}{8}\sqrt{\frac{a}{2k\det\operatorname{Im}\boldsymbol{\Gamma}_0^{-1}}}\left(\frac{1}{\lambda_2}-\frac{1}{\lambda_1}\right), \tag{93}$$

where $\lambda_1 > \lambda_2 > 0$ and $\mu_1 > \mu_2$ are eigenvalues of the matrices $-\operatorname{Im}\boldsymbol{\Gamma}_0^{-1}$ and $\operatorname{Re}\boldsymbol{\Gamma}_0^{-1}$, respectively, and $\varkappa$ is the angle between the eigenvectors corresponding to λ_1 and μ_1.

It is remarkable that in contrast to the results for energy (77) and momentum (78), the expression (93) does not depend on the tilt angle ϕ. Also noteworthy is the fact that the value of OAM (93) is proportional to $k^{-1/2}$, while (77) and (78) are proportional to $k^{1/2}$.

IX. Discussion

We have obtained closed-form expressions for scalar tilted non-paraxial waveobjects. The derivation was done in two ways, showing that complex shifts and Lorentz transformations of Bateman-type expressions lead to the same class of solutions of the wave equation. The solutions found can, in particular, be used for builiding new localized solutions by integrating with appropriate weights over the shift parameter, generalizing a construction presented in [9] for simple astigmatism in the paraxial case.

We have also derived the analytical expressions of the propagation invariants of the scalar wave equation for the tilted waveobjects, including those with general astigmatism. These results give the energy, momentum and angular momentum of tilted sound waves in a straightforward manner, via the simple application of the factor ρ_0, the density of the unperturbed fluid.

Even though sound and electromagnetic wave phenomena display strong contrasts in their structural physical properties: scalar versus vectorial, oscillations that are longitudinal to the propagation axis in contrast to transverse, the first requiring a material support and the second not, they are both described by the same fundamental mathematical apparatus: the wave

equation (1). In the case of electromagnetic waves, a full vector treatment requires to establish a precise relation between the scalar and the full vector electromagnetic problems. For instance, the scalar wavefunction can be set as one component of the vector potential [26].

Light carries both spin angular momentum (SAM) and OAM. Whereas SAM is associated to its polarization state, OAM is linked to the phase structure of the optical field. OAM is best described using the canonical momentum density [27], which is proportional to the local gradient of the phase of the field. While spin is intrinsic to the vector characteristics of the fields, the orbital momentum density can be defined equally for vector or scalar optical waveobjects [27], [28].

The conserved quantities presented in this work apply in general to the solutions of the wave equation with independence of their physical context. Nevertheless, the momentum density in scalar optics is normally treated as the optical current [28]

$$\boldsymbol{\mathcal{P}} = \operatorname{Im} u^* \nabla u \tag{94}$$

from which the angular momentum density is $\boldsymbol{\mathcal{J}} = \mathbf{R} \times \boldsymbol{\mathcal{P}}$. The optical current of Equation (94) has also been shown to correspond to the nonzero cycle-averaged part of the momentum density of the scalar waveobject u [29]. It can be recognized as a normalized form of the momentum density in the quantum domain, where u is the quantum wavefunction and the conventions for the scalar conserved quantities for photons and phonons meet.

Even though light carrying OAM is often structured as an optical vortex, solutions of the wave equation with general astigmatism [5], [19] can hold very large values of OAM yet they lack wavefront singularities [30]–[32]. The family of the tilted waves presented here encompasses this class of astigmatic beams and packets with distinct OAM spectral properties that open many highly interesting potential applications in quantum physics and quantum communications driven by OAM management. These include the engineering of multidimensional photon states and the generation of entangled photons with very large OAM quantum numbers for improved sensitivy quantum metrology and the exploration of the quantum limits of the information capacity of OAM photonic carriers and quantum-classical coupling [31].

The role played by Lorentz transformations in the inception of tilted waveobjects unveiled in this work makes these solutions specially appealing form the viewpoint of the rapidly growing interest on the properties of waveobjects carrying AM under relativistic transformations [33]. This includes fundamental questions like the AM-dependent transverse shift in the relativistic Hall effect [34] or the scattering of high-energy OAM-carrying waveobjects [33] and it is also notably relevant in relation to the recent burst of spatiotemporal vortex pulses and the interest raised on their AM properties when they are subject of Lorentz transformations [35]. In this work, we put forward OAM-carrying spatiotemporal tilted pulses with general astigmatism, of a markedly distinct type of related solutions previously studied [33], [35], whose propagation properties are dictated by relativistic transformations.

ACKNOWLEDGMENT

Authors are indebted to Maria Perel for a helpful discussion and to the anonymous reviewer for constructive comments.

APPENDIX
A. A DETAILED DERIVATION OF A CONVENIENT REPRESENTATION OF THE FUNCTION (16)

We are now going to derive a representation of the phase function (16) suitable for further interpretation. Its structure is prompted by earlier research [9], [13] which addressed particular cases of the general astigmatic solution.

The second item in Eq. (16) is a complex-valued quadratic form of a complex matrix $\boldsymbol{\Gamma}(\beta)$ on a complex vector $\mathbf{r} - \mathbf{r}^*$. Inspired by earlier study of particular cases, we are seeking its representation in the form (17) where

$$\theta_2 = \theta_2(\mathbf{r}, \beta) = (\mathbf{r} - \breve{\mathbf{r}}(\beta))^T \boldsymbol{\Gamma}(\beta)(\mathbf{r} - \breve{\mathbf{r}}(\beta)) \tag{95}$$

is the value of the quadratic form of the matrix $\boldsymbol{\Gamma}(\beta)$ on a yet unknown real vector $\breve{\mathbf{r}}$ chosen in such a way that $\theta_1 = \theta_1(\mathbf{r}, \beta)$ is a real and linear both in $\mathbf{r}$ and in β. With this in view, we seek the vector $\mathbf{r} - \mathbf{r}^*$ as a sum

$$\mathbf{r} - \mathbf{r}^* = (\mathbf{r} - \breve{\mathbf{r}}(\beta)) + (\breve{\mathbf{r}}(\beta) - \mathbf{r}^*)\,,$$

with the first item real and the second satisfying the requirement that the vector defined as

$$\boldsymbol{\kappa} = \boldsymbol{\Gamma}(\beta)(\breve{\mathbf{r}}(\beta) - \mathbf{r}^*)\,. \tag{96}$$

is real. Actually, (96) is equivalent to

$$\boldsymbol{\Gamma}^{-1}(\beta)\boldsymbol{\kappa} = \breve{\mathbf{r}}(\beta) - \mathbf{r}^*\,,$$

whence, since $\breve{\mathbf{r}}$ is assumed real,

$$\operatorname{Im} \boldsymbol{\Gamma}^{-1}\boldsymbol{\kappa} = -\operatorname{Im} \mathbf{r}^*\,,$$

and

$$\operatorname{Re} \boldsymbol{\Gamma}^{-1}(\beta)\boldsymbol{\kappa} = \breve{\mathbf{r}}(\beta) - \operatorname{Re} \mathbf{r}^*\,.$$

According to (5), the matrix $\operatorname{Im} \boldsymbol{\Gamma}^{-1} = \operatorname{Im} \boldsymbol{\Gamma}_0^{-1}$ is constant, non-degenerate and negative definite whence the vector

$$\boldsymbol{\kappa} = -(\operatorname{Im} \boldsymbol{\Gamma}^{-1})^{-1} \operatorname{Im} \mathbf{r}^* = -(\operatorname{Im} \boldsymbol{\Gamma}_0^{-1})^{-1} \operatorname{Im} \mathbf{r}^* \tag{97}$$

is independent of β. Making use of (5), we obtain

$$\tilde{\mathbf{r}}(\beta) = \operatorname{Re} \mathbf{r}^* + (\operatorname{Re} \boldsymbol{\Gamma}_0^{-1} + \beta \mathbf{I})\boldsymbol{\kappa}\,. \tag{98}$$

A straightforward calculation employing (97) and (98) allows

$$(\mathbf{r} - \mathbf{r}^*)^T \boldsymbol{\Gamma}(\beta)(\mathbf{r} - \mathbf{r}^*) = (\mathbf{r} - \breve{\mathbf{r}}(\beta))^T \boldsymbol{\Gamma}(\beta)(\mathbf{r} - \breve{\mathbf{r}}(\beta)) + 2\boldsymbol{\kappa}^T(\mathbf{r} - \breve{\mathbf{r}}(\beta)) + \boldsymbol{\kappa}^T(\boldsymbol{\Gamma}_0^{-1} + \beta \mathbf{I})\boldsymbol{\kappa}.$$

which defines in fact the desired representation (17).

To give it a convenient form, we introduce a couple of notations. Introduce a constant vector by

$$\mathbf{r}_0 = \operatorname{Re} \mathbf{r}^* + \operatorname{Re} \boldsymbol{\Gamma}_0^{-1} \boldsymbol{\kappa}\,,$$

Let

$$\boldsymbol{\kappa} = \boldsymbol{\tau} |\boldsymbol{\kappa}| \tag{99}$$

where

$$\boldsymbol{\tau} = \frac{\boldsymbol{\kappa}}{|\boldsymbol{\kappa}|} = -\frac{(\operatorname{Im}\boldsymbol{\Gamma}_0^{-1})^{-1}\operatorname{Im}\mathbf{r}^*}{|(\operatorname{Im}\boldsymbol{\Gamma}_0^{-1})^{-1}\operatorname{Im}\mathbf{r}^*|} \tag{100}$$

is a unit vector along $\boldsymbol{\kappa}$, and

$$|\boldsymbol{\kappa}| = \tan\phi\,, \tag{101}$$

or

$$\phi = \arctan|\boldsymbol{\kappa}| = \arctan|(\operatorname{Im}\boldsymbol{\Gamma}_0^{-1})^{-1}\operatorname{Im}\mathbf{r}^*|\,. \tag{102}$$

Now the items on the right-hand side of Eq. (17) can be written as follows

$$\theta_2 = (\mathbf{r}-\mathbf{r}_0-\boldsymbol{\kappa}\beta)^T\boldsymbol{\Gamma}(\beta)(\mathbf{r}-\mathbf{r}_0-\boldsymbol{\kappa}\beta) = (\mathbf{r}-\mathbf{r}_0-\beta\boldsymbol{\tau}\tan\phi)^T\boldsymbol{\Gamma}(\beta)(\mathbf{r}-\mathbf{r}_0-\beta\boldsymbol{\tau}\tan\phi)\,, \tag{103}$$

$$\theta_1 = \alpha + 2\boldsymbol{\kappa}^T(\mathbf{r}-\mathbf{r}_0) - |\boldsymbol{\kappa}|^2\beta = z(1-|\boldsymbol{\kappa}|^2) + 2\boldsymbol{\kappa}^T(\mathbf{r}-\mathbf{r}_0) - ct(1+|\boldsymbol{\kappa}|^2) = \frac{z\cos 2\phi + \boldsymbol{\tau}^T(\mathbf{r}-\mathbf{r}_0)\sin 2\phi - ct}{\cos^2\phi}\,, \tag{104}$$

and

$$\theta_0 = \boldsymbol{\kappa}^T\boldsymbol{\Gamma}_0^{-1}\boldsymbol{\kappa}\,. \tag{105}$$

The term (105) has negative imaginary part because $\operatorname{Im}\boldsymbol{\Gamma}_0^{-1}$ is negative definite.

Appendix
B. Asymptotic derivation of the integral I_1

Substitution of (71) into (86) gives the appoximation

$$I_1 \approx -k^2h_0^5\iint_{\mathbb{R}^2}\chi^2(\boldsymbol{\psi}_0^T\operatorname{Re}\boldsymbol{\Gamma}_0^{-1}\boldsymbol{\psi}_0)_\varphi \times\exp\left(2kh_0^2\chi^2\boldsymbol{\psi}_0^T\operatorname{Im}\boldsymbol{\Gamma}_0^{-1}\boldsymbol{\psi}_0\right)\,\chi d\chi d\varphi \times\int_{-\infty}^{\infty}\exp\left(-2kh_0^2s^2/a\right)\,ds\,. \tag{106}$$

By the formula (74), the integral over s equals $\sqrt{\pi a/2k}/h_0$. Now we will represent the expression $(\boldsymbol{\psi}_0^T\operatorname{Re}\boldsymbol{\Gamma}_0^{-1}\boldsymbol{\psi}_0)_\varphi$ as a quadratic form of a certain matrix $\mathbf{Q}$. Noticing that

$$\partial_\varphi\boldsymbol{\psi}_0 = (-\sin\varphi\,,\cos\varphi)^T = \mathbf{V}\boldsymbol{\psi}_0\,,\quad \partial_\varphi\boldsymbol{\psi}_0^T = -\boldsymbol{\psi}_0^T\mathbf{V}\,,$$

where $\mathbf{V} = \begin{pmatrix}0 & -1\\ 1 & 0\end{pmatrix}$, we get:

$$\partial_\varphi[\boldsymbol{\psi}_0^T\operatorname{Re}\boldsymbol{\Gamma}_0^{-1}\boldsymbol{\psi}_0] = \boldsymbol{\psi}_0^T\mathbf{Q}\boldsymbol{\psi}_0$$

with $\mathbf{Q} = \operatorname{Re}\boldsymbol{\Gamma}_0^{-1}\mathbf{V} - \mathbf{V}\operatorname{Re}\boldsymbol{\Gamma}_0^{-1}$.

Let us change the variables χ and φ to $\xi = \sqrt{2k}h_0\chi\cos\varphi$ and $\eta = \sqrt{2k}h_0\chi\sin\varphi$. Next, we introduce the vector $\boldsymbol{\zeta} = (\xi\,,\,\eta)^T$ and extend the integration with respect to ξ and η to the whole plane $\mathbb{R}^2$. The integral under consideration becomes

$$I_1 \approx -\frac{1}{4}\sqrt{\frac{\pi a}{2k}}\iint_{\mathbb{R}^2}\boldsymbol{\zeta}^T\mathbf{Q}\boldsymbol{\zeta}\,\exp\left(-\boldsymbol{\zeta}^T\mathbf{A}\boldsymbol{\zeta}\right)\,d^2\boldsymbol{\zeta}\,, \tag{107}$$

where we denoted for brevity $\mathbf{A} = -\operatorname{Im}\boldsymbol{\Gamma}_0^{-1}$.

Without loss of generality, we assume that the positive definite matrix $\mathbf{A}$ is diagonal,

$$\boldsymbol{\zeta}^T\mathbf{A}\boldsymbol{\zeta} = \lambda_1\xi^2 + \lambda_2\eta^2\,, \tag{108}$$

and $\lambda_1 > \lambda_2 > 0$ (this can be achieved by rotating the coordinate axes in the (ξ,η) plane). Denote by $\mu_1 > \mu_2$ the eigenvalues of $\mathbf{B} = \operatorname{Re}\boldsymbol{\Gamma}_0^{-1}$. The following representation for $\mathbf{B}$ holds true

$$\mathbf{B} = \frac{\mu_1+\mu_2}{2}\mathbf{I} + \frac{\mu_1-\mu_2}{2}\begin{pmatrix}\cos 2\varkappa & \sin 2\varkappa\\ \sin 2\varkappa & -\cos 2\varkappa\end{pmatrix}\,, \tag{109}$$

where $\mathbf{I}$ is the unit matrix, $\varkappa$ is the angle between those eigenvectors of the matrices $\mathbf{A}$ and $\mathbf{B}$ that correspond to their largest eigenvalues λ_1 and μ_1. Simple calculation shows that

$$\mathbf{Q} = \mathbf{B}\mathbf{V} - \mathbf{V}\mathbf{B} = -(\mu_1-\mu_2)\begin{pmatrix}-\sin 2\varkappa & \cos 2\varkappa\\ \cos 2\varkappa & \sin 2\varkappa\end{pmatrix}\,,$$

whence

$$\boldsymbol{\zeta}^T\mathbf{Q}\boldsymbol{\zeta} = -(\mu_1-\mu_2)\left[\sin 2\varkappa(-\xi^2+\eta^2) + 2\cos 2\varkappa\cdot\xi\eta\right]\,. \tag{110}$$

After observing that the integral of the last term in square brackets on the right side of (110) vanishes and the use of (108) and (110), we obtain from (107):

$$I_1 \approx \sqrt{\frac{\pi a}{2k}}\frac{(\mu_1-\mu_2)\sin 2\varkappa}{4} \times\left\{-\int_{-\infty}^{\infty}\xi^2\exp(-\lambda_1\xi^2)\,d\xi\int_{-\infty}^{\infty}\exp(-\lambda_2\eta^2)\,d\eta + \int_{-\infty}^{\infty}\exp(-\lambda_1\xi^2)\,d\xi\int_{-\infty}^{\infty}\eta^2\exp(-\lambda_2\eta^2)\,d\eta\right\}.$$

Applying the formula $\int_{-\infty}^{\infty}\sigma^2\exp(-m^2\sigma^2)\,d\sigma = \sqrt{\pi}/2m^3$ (see, e.g., [36]) together with (74), we find

$$J \approx \frac{1}{c}\frac{\pi^{3/2}(\mu_1-\mu_2)\sin 2\varkappa}{8}\sqrt{\frac{a}{2k\lambda_1\lambda_2}}\left(\frac{1}{\lambda_2}-\frac{1}{\lambda_1}\right) \tag{111}$$

The last expression is the same as (93) because $\lambda_1\lambda_2 = \det\operatorname{Im}\boldsymbol{\Gamma}_0^{-1}$.

We note that the formula (111) for the integral (93) is similar to the one given in [32] without a commentary.

References

[1] J. N. Brittingham, "Focus waves modes in homogeneous Maxwell's equations: Transverse electric mode," J. Appl. Phys., vol. 54, pp. 1179–1189, 1983.

[2] A.P. Kiselev and M.V. Perel, "Gaussian wave packets," Opt. Spectros., vol. 86, no. 3, pp. 307 – 309, 1999.

[3] A.P. Kiselev and M.V. Perel, "Highly localized solutions of the wave equation," J. Math. Phys., vol. 41, pp. 1934–1955, 2000.

[4] A.P. Kiselev, "Localized light waves: Paraxial and exact solutions of the wave equation (a review)," Opt. Spectrosc., vol. 102, pp. 603 – 622, 2007.

[5] A.P. Kiselev, A.B. Plachenov and P. Chamorro-Posada, "Nonparaxial wave beams and packets with general astigmatism," Phys. Rev. A, vol. 85, 2012, Art. no. 043835.

[6] Y. Hadad and T. Melamed, "Non-Orhtogonal Domain Parabolic Equation and Its Tilted Gaussian Beam Solutions," IEEE Trans. Antennas Propag., vol. 58, no. 4, pp. 1164–1172, 2010.

[7] Y. Hadad and T. Melamed, "Parametrization of the tilted Gaussian beam waveobjects," Prog. Electromagn. Res., vol. 102, pp. 65–80, 2010.

[8] Y. Hadad and T. Melamed, "Time-Dependent Tilted Pulsed-Beams and Their Properties," IEEE Trans. Antennas Propag., vol. 59, no. 10, pp. 3855–3862, 2011.

[9] A.B. Plachenov, I.A. So, and A.P. Kiselev, "Paraxial Gaussian modes with simple astigmatic phases and nonpolynomial amplitudes," in *Proc. Intern. Conf. Days on Diffraction 2017*, *IEEE*, 2017, pp. 264 – 269.

[10] P. Hillion, "The Courant–Hilbert solutions of the wave equations," J. Math. Phys., vol. 33, pp. 2749–2752, 1992.

[11] H. Bateman, "The transformation of the electrodynamical equations," Proc. London Math. Soc., vol. 8, pp. 223–264, 1910.

[12] H. Bateman, *The Mathematical Analysis of Electrical and Optical Wave-Motion*, Cambridge: Cambridge University Press, 1915.

[13] A.B. Plachenov, "Tilted nonparaxial beams and packets for the wave equation with two spatial variables," J. Math. Sci., vol. 185, no. 4, pp. 738–644, 2011.

[14] A.P. Kiselev, A.B. Plachenov, and P. Chamorro-Posada, "Further generalizations of the Bateman solution. Novel wave beams and wave packets," in *Days on Diffraction'2012. International Conference. SPb, Russia, May 28 - June 1, 2012. Proceedings*, pp. 124-128.

[15] Kiselev A. P., "New structures in paraxial Gaussian beams," Opt. Spectrosc., vol. 96, no. 4, pp. 533 – 535, 2004.

[16] A. P. Kiselev, "Generalization of Bateman–Hillion progressive wave and Bessel-Gauss pulses solutions of the wave equation via a separation of variables," J. Phys. A: Math. Gen., vol. 36, no. 23, pp. L345 – L349, 2003.

[17] M. Perel and E. Gorodnitskiy, "Integral representations of solutions of the wave equation based on relativistic wavelets," J. Phys. A: Math. Theor., vol. 45, 2012, Art. no. 385203.

[18] R. Courant and D. Hilbert, *Methods of Mathematical Physics*, Vol. 2, New York: Interscience, 1962.

[19] J. A. Arnaud and H. Kogelnik, "Gaussian Light Beams with General Astigmatism," Appl. Opt., vol. 8, pp. 1687–1693, 1969.

[20] A.P. Kiselev, A.B. Plachenov, and G.N. Dyakova, "On the analyticity of waveforms in complexified relatively undistorted progressing waves," J. Electromagnetic Waves and Applications, vol. 31, no. 13, pp. 1325 – 1332, 2017.

[21] E. C. Titchmarsh, *The Theory of Functions*, Oxford University Press, 1939.

[22] L. D. Landau and E. M. Lifshitz, *The Classical Theory of Fields*, Oxford, Pergamon, 1971.

[23] L. D. Landau and E. M. Lifshitz, *Fluid Mechanics*, Oxford, Pergamon, 1987.

[24] J. Lekner "Energy, momentum, and angular momentum of sound pulses," J. Acoust. Soc. Amer., vol. 142, 2017, pp. 3428–3435.

[25] R. Wong, *Asymptotic Approximation of Integrals*, Philadelphia: SIAM, 2001.

[26] J. Lekner "Energy and momentum of electromagnetic pulses," J. Opt. A: Pure Appl. Opt., vol. 6, 2004, pp. 146–147.

[27] K.Y. Bliokh and F. Nori, "Transverse and longitudinal angular momenta of light," Phys. Rep., vol. 592, pp. 1–38, 2015.

[28] M.V. Berry, "Optical currents," J. Opt. A: Pure Appl. Opt., vol. 11, 2009, Art. no. 094001.

[29] J. Lekner, "Acoustic beams with angular momentum," J. Acoust. Soc. Am., vol. 120, 2006, 2475–3478.

[30] J. Courtial, K. Dholakia, L. Allen, and M.J. Padgett, "Gaussian beams with very high orbital angular momentum," Opt. Commun., vol. 144, pp. 210–213, 1997.

[31] A.B. Plachenov, P. Chamorro-Posada, and A.P. Kiselev, "Quadratic Bessel-Gauss beams and the azimuthal angular spectra of Gaussian astigmatic beams," Phys. Rev. A, vol. 102, 2020, Art. no. 023533.

[32] J. Visser and G. Nienhuis, "Orbital angular momentum of general astigmatic modes," Phys. Rev. A, vol. 70, 2004, Art. No. 013809.

[33] D.A. Smirnova, V.M. Travin, K.Y. Bliokh, and F. Nori, "Relativistic spin-orbit interactions of photons and electrons," Phys. Rev. A, vol. 97, 2018, Art. no. 043840.

[34] K.Y. Bliokh and F. Nori, "Relativistic Hall Effect," Phys. Rev. Lett., vol. 108, 2012, Art. no. 120403.

[35] K.Y. Bliokh, "Spatiotemporal Vortex Pulses: Angular Momenta and Spin-Orbit Interaction," Phys. Rev. Lett, vol. 126, 2021, Art. no. 243601.

[36] H.B. Dwight, *Tables of Integrals and Other Mathematical Data*, New York: Macmillan, 1961.